

R. Drobñjak
High Technical School Uzice

A. Sedmak
Professor

V.Šijački-Žeravčić
Professor

A. Milosavljević
Professor
University of Belgrade
Faculty of Mechanical Engineering

Numerical Simulation of Quenching Process

II Part: Residual Stresses

Starting from the basic laws of continuum mechanics, the procedure of finite element method application to the quenching residual stresses evaluation is defined, taking as input data spatial and time distribution of temperature, obtained in the first part of paper. As an application of this procedure, two examples of calculation of residual stresses due to cylinder quenching are given, in one case without phase transformation, and in the other one with phase transformation of austenite - bainite type.

Keywords: Quenching, Residual Stresses, Finite Element Method.

1. INTRODUCTION

As shown in the first part of this paper [1], quenching is characterized by large and rapid temperature changes, followed by phase transformations in materials such as steel. As a consequence, residual stresses and crack-like defects may appear. Although many papers have been devoted to the theoretical, experimental and numerical investigation of quenching, these problems have not been solved yet. Therefore, a state-of-the-art is given in this paper, based on reference [2], including numerical evaluation of residual stresses, based on time and spatial distribution of temperature during quenching, given in [3]. Toward this end stress problem is defined by the partial differential equations, derived in the scope of basic laws of continuum mechanics, which are solved by the finite element method.

2. THEORETICAL ANALYSIS OF RESIDUAL STRESSES

Residual stresses are defined here as the thermal stresses caused by a non-uniform cooling of a quenched part and the influence of phase transformation is analysed later. More detailed explanation is given in Fig. 1, where three characteristic sections (A-A, B-B and C-C) show the spatial and time distribution of radial, axial and circumference stress during quenching. The section A-A is along the outer surface of quenched part (taken here to be of a cylindrical shape), where the cooling is the fastest, section C-C contains the central cylinder axis, where the cooling is the slowest, and section B-B is in between, Fig. 1. The stress distribution is a consequence of thermal contraction of the material next to the coolant (spray water), being suppressed by surrounding hot material. In this way, the compression

stresses are generated in the material next to the coolant, balanced by the remote tensile stresses. Only radial stress does not invert from tension in section C-C to pressure in section A-A, but rather reduces to zero, because there is no surrounding material along r axis to produce such a distribution.

It should be noted that stresses at high temperature are practically zero, because no resistance to the thermal forces is provided. Gradual increase of stresses with temperature decrease is due to increased material resistance to the thermal forces.

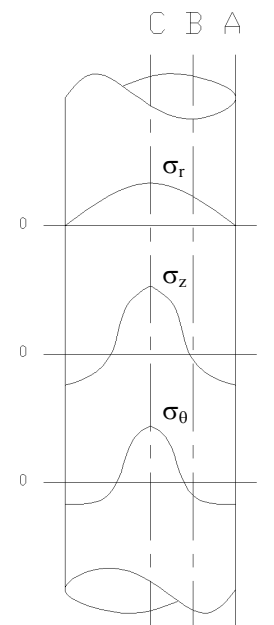


Figure 1. Residual stress distribution in quenched cylinder

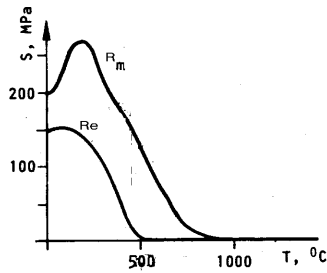
Dependence of material properties on temperature is given for a typical structural steel in Fig. 3a (yield stress and tensile strength), Fig. 3b (elasticity modulus), Fig. 3c (Poisson's ratio) and Fig. 3d (linear thermal expansion coefficient), [3]. As already stated, the yield stress and elasticity modulus reduce as temperature rises, so that yield stress is practically zero at 500°C, while mate-

Received: January 2001, accepted: February 2002.

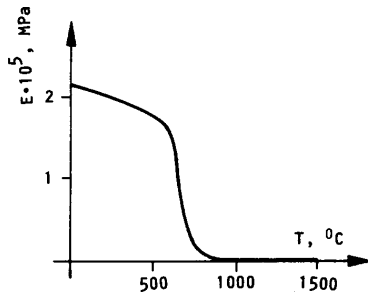
Correspondence to:

Aleksandar Sedmak, Faculty of Mechanical Engineering,
27. marta 80, 11000 Belgrade, Yugoslavia

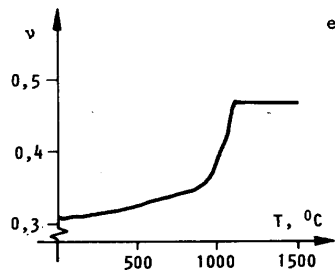
rial stiffness disappears at 700°C (elasticity modulus is 0). These temperatures are material dependent, but for the ordinary structural steels they can serve as the first approximation.



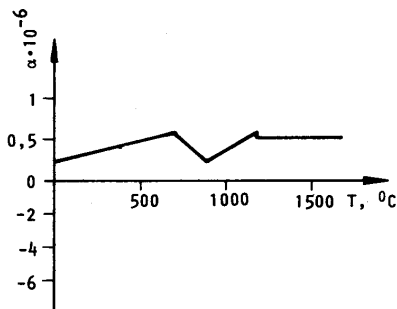
a) yield stress and tensile strength



b) elasticity modulus



c) Poisson's ratio



d) linear thermal expansion coefficient

Figure 2. Material characteristics vs. temperature

3. APPLICATION OF FINITE ELEMENT METHOD

In the part I of this paper, [1], the finite element method application to the heat conduction problem has been analysed, where this method was introduced as the universal numerical method for solving non-linear non-stationary partial differential equation. The basic procedure of finite element method application for residual stresses evaluation is essentially the same as for

the heat conduction problem and includes domain discretization (division into finite elements), interpolation of all quantities inside finite elements, integration over all elements and solution of the resulting equation system. The basic difference are the equations to be solved because the independent variable in residual stress problem is displacement instead of temperature, the static equilibrium equations are to be solved instead of heat conduction equations and material behaviour is described by the stress-strain relation instead of using the Fourier's law. Thereby it is necessary to introduce the isoparametric interpolation functions for displacements as follows:

$$u^i(x^j, t) = N^K(x^j) u_K^i(t), \quad (1)$$

where $u^i(x^j, t)$ denotes temperature distribution inside element, $N^K(x^j)$ interpolation function, $u_K^i(t)$ nodal displacement and x^j Descartes coordinates. Now, one can write:

$$\varepsilon_{kl} = \frac{\partial u^k}{\partial x^l} = \frac{\partial N^K}{\partial x^l} u_K^k = N_{\ell}^K u_K^k, \quad (2)$$

where N_{ℓ}^K denotes matrix of $n \times r$ order (n is the space dimension and r the number of elements). Geometrical non-linearity has been neglected as a reasonable assumption for the problem considered. On the other hand, material non-linearity can not be neglected, leading to the expression for incremental strain comprising elastic, plastic and thermal component:

$$d\varepsilon_{kl} = d\varepsilon_{kl}^e + d\varepsilon_{kl}^{ep} + \delta_{kl} d\varepsilon^T, \quad (3)$$

The elastic strain can be related to the stress by the following equation (Hooke's law):

$$d\sigma_{ij} = E_{ijkl} d\varepsilon_{kl}^e, \quad (4)$$

where $d\sigma_{ij}$ denotes stress tensor increment and E_{ijkl} elasticity tensor. The plastic strain can be expressed using the incremental plasticity theory, taking into account normality condition, Von Mises yield criterion and material strain strengthening assumption:

$$d\varepsilon_{ij}^p = \frac{3}{2} \frac{d\varepsilon_e^p}{\sigma_e} S_{ij}, \quad (5)$$

where S_{ij} denotes stress deviator tensor, and $d\varepsilon_{ij}^p$ and σ_e denote the equivalent plastic strain increment and stress, respectively, given by:

$$\sigma_e = \sqrt{\frac{3}{2} S_{ij} S_{ij}}; \quad d\varepsilon_e^p = \sqrt{\frac{2}{3} d\varepsilon_{ij}^p d\varepsilon_{ij}^p}, \quad (6)$$

If the transformation plasticity is neglected, the thermal strain $d\varepsilon^T$ can be expressed as follows:

$$d\varepsilon^T = \alpha dT, \quad (7)$$

where α denotes coefficient of linear thermal expansion, and dT temperature change. For ordinary structural steel, when there is no martensitic transformation during welding, transformation plasticity can be neglected, while in the opposite case Eqn (7) should be modified by adding the appropriate term, as shown in [4]:

$$d\varepsilon^T = \alpha dT + k' dm, \quad (8)$$

where dm denotes martensite volume content, generated by temperature change, k' material constant, equal to $0,011 \text{ K}^{-1}$ for most structural steels, [4].

4. EXAMPLES

Two examples are chosen to illustrate the procedure described above, both of them related to the cylinder quenching. In the first example pure iron cylinder ($\phi 50 \text{ mm}$) is analysed in order to verify the basic numerical procedure (excluding phase transformations), and also to explain the discrepancies obtained by two different experimental methods, as described in more details in [5]. Namely, the hole drilling technique (line A, Fig. 3) and slicing of cylinder (line B, Fig. 3), produced significantly different results. It has been assumed, and indeed proved by the finite element analysis, that plastic strains have occurred during the experiment, violating the basic condition for the hole drilling technique, explaining thus the differences both between the two experiments and also between experimental and numerical results, given by line C, Fig. 3. More detailed analysis, including finite elements being plastified during this process, is given in [1].

Material data necessary for calculation is given in Tab. 1. The finite element mesh is the same as shown in [1], with the boundary conditions prescribed on all surfaces, except the outer one, where the experimentally obtained results are prescribed.

Table 1. Mechanical properties of pure iron

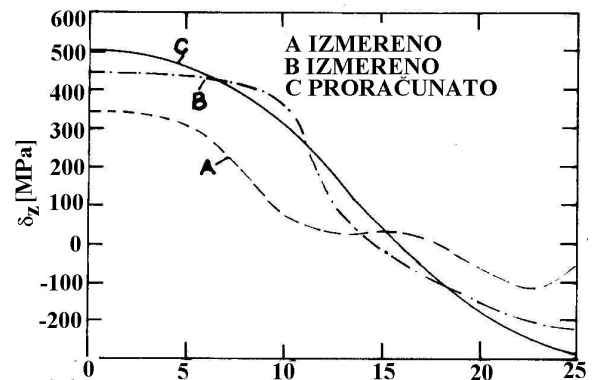
T (°C)	E (GPa)	ν	R_{eh} (MPa)	H (GPa)	α (10^{-5}K^{-1})
20	208	0,290	190	6,8	1,46
200	198	0,262	173	12,1	1,52
300	190	0,265	103	16,3	1,55
500	173	0,291	67	5,3	1,59
600	164	0,307	55	2,4	1,6
700	153	0,329	27	9	1,6
900	128	0,379	15	1	1,6

Table 2. Mechanical properties of CrMoV steel

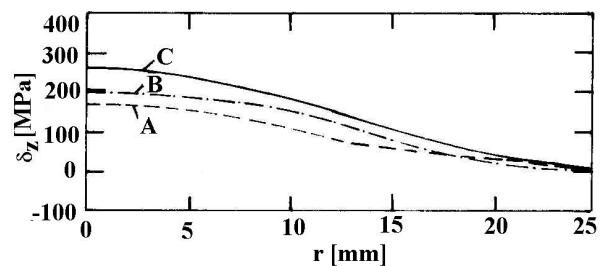
T (°C)	E (GPa)	R_{eh} (MPa)		α (10^{-5}C^{-1})	
		A	B	A	B
20	205		860		1,1
100	201		860		1,1
150	198		860		1,1
200	194	105	860	2,1	1,1
400	173	95	860	2,1	1,1
600	145	85	860	2,3	1,1
800	115	60		2,5	
1000	85	20		2,5	

A - austenite, B - bainite; $H=0,05E$ (MPa)

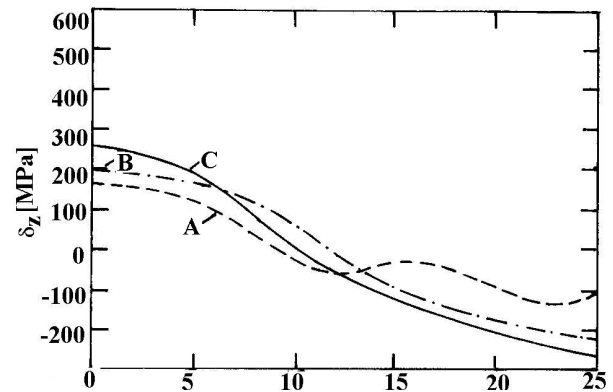
In the second example a large shaft ($\phi 1310 \text{ mm}$), made of CrMoV steel is analysed, [6]. Mechanical properties for CrMoV steel are given in Tab. 2, including bainite and austenite structure properties, given at appropriate temperatures.



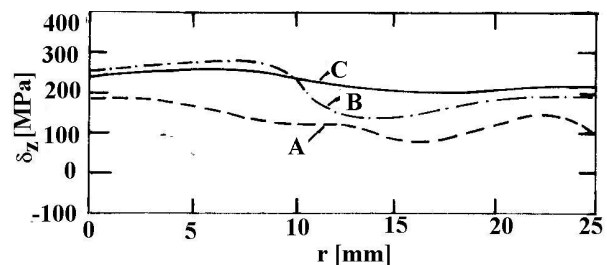
a) axial stress component



b) radial stress component



c) tangential stress component



d) equivalent stress

Figure 3. Residual stresses for quenched cylinder

The finite element mesh is same as in the previous example, and the boundary conditions are shown in Fig. 3.

Three different variants of calculation were performed (marked by 1-3 in Fig. 5 and 6, respectively):

1. without martensite transformation;
2. with transformation plasticity, but without volume transformation;
3. with complete martensite transformation.

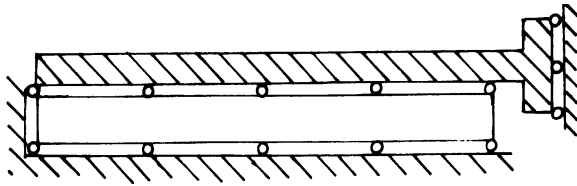


Figure 4. Modeling of cylinder $\phi 1310$

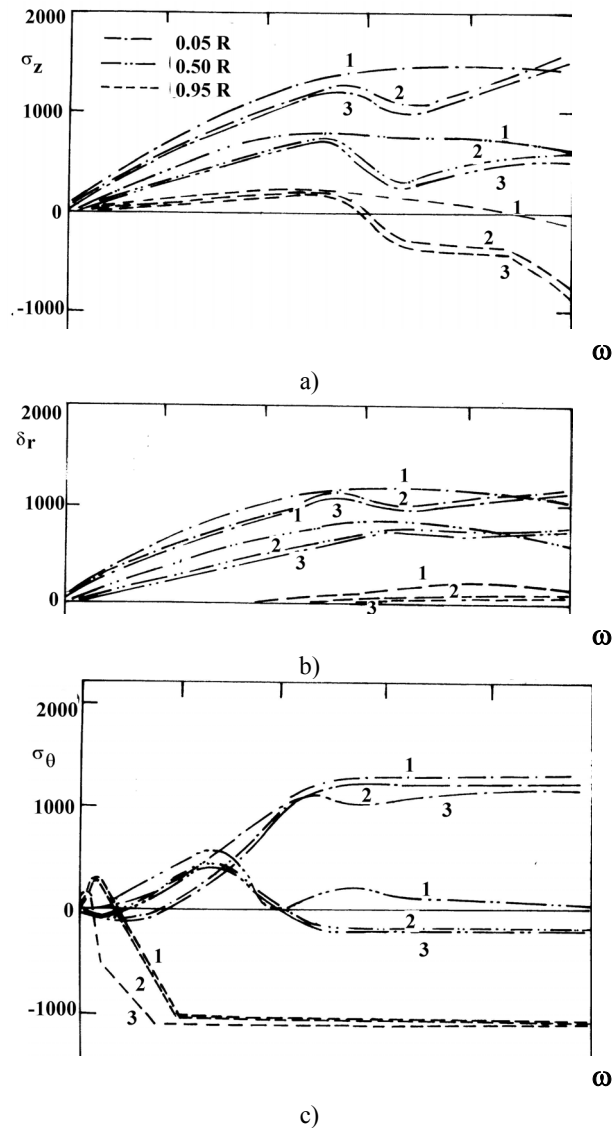


Figure 5. Results for residual stresses

Data used for the second variant of calculation was: coefficient of proportionality $k'=0,0038 \text{ }^\circ\text{C}^{-1}$, parameters $b_k=-6$, $n_k=2$, [6]. The coefficient K, needed for the third variant of calculation was assumed to be $K=5,2 \cdot 10^{-5} \text{ mm}^2/\text{N}$, [6]. By applying these values, the results for residual stresses and equivalent plastic strain are obtained as shown in Fig. 5 and Fig. 6, respectively, for

three different position in cylinder ($0.05 \cdot R$, $0.50 \cdot R$ and $0.95 \cdot R$, where R stands for the cylinder radius). The results for residual stresses are plotted against non-dimensional temperature parameter $\omega=(T_i-T)/(T_i-T_f)$, where T_i stands for the initial temperature and T_f for the final one, Fig. 5, whereas equivalent strain is plotted against time, Fig. 6.

As one can see from Fig. 5 and 6, significant difference in residual stresses and equivalent strain distribution appears if transformation plasticity and/or volume transformation is taken into account (variants 2 and 3), while only slight difference is noticeable between the results for variants 2 and 3. Therefore, it is clear that in this case, the transformation plasticity is much more influential than the volume transformation.

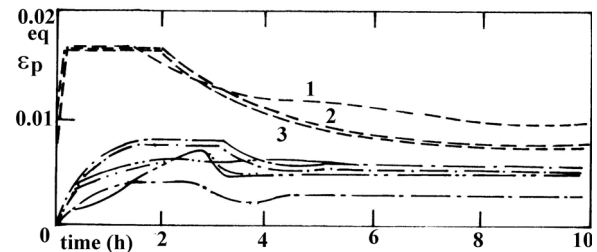


Fig. 6. The equivalent plastic strain

5. DISCUSSION AND CONCLUSIONS

The finite element modeling of quenching process has proved to be successful for residual stresses calculation, as shown by two examples of cylinder quenching. The basic numerical procedure (without phase transformation) has been verified by the first example, where the results of numerical simulation shown good agreement with the experimental results, obtained by surface slicing method, whereas the second example has shown good agreement with the other numerical results, including the influence of phase transformation. It has been shown that the transformation plasticity is much more influential than the volume transformation when residual stresses and equivalent strain due to quenching are analysed.

REFERENCES

- [1] Drobñjak R., Sedmak A., Šijacki-Žeravčić V., Milosavljević A.: Numerical simulation of quenching process - I part: temperature fields, Transactions, Vol. 29, pp. 20-24, Faculty of Mechanical Engineering, University of Belgrade, 1999.
- [2] Drobñjak R.: *Analysis of processes with phase and state transformation - casting, quenching and welding* (in serbian), doctoral thesis, Faculty of Mechanical Engineering, University of Belgrade, 1997.
- [3] Berković M., Maksimović S., Sedmak Aa., Analysis of welded joints by the finite element method (in serbian), Proc. III International Fracture Mechanics Summer School, Arandelovac, GOŠA-TMF, p. 111-128, 1984.

- [4] Denis S., Gautier E., Simon A., Beck G., Stress-phase transformation interactions - basic principles, modelling, and calculation of internal stresses, *Material Science and Technology*, Vol. 1, p. 805-813, 1985.
- [5] Mitter W., Rammersstorfer F.G., Grundler O., Wiedner G., Discrepancies between calculated and measured residual stresses in quenched pure iron cylinder, *Material Science and Technology*, Vol. 1, p. 793-797, 1985.
- [6] Kamamoto S., Nishimori T., Kinoshito S., Analysis of residual stress and distortion resulting from quenching in large low-alloy steel shafts, *Material Science and Technology*, Vol. 1, p. 798-804, 1985.
-

НУМЕРИЧКА СИМУЛАЦИЈА ПРОЦЕСА КАЉЕЊА II ДЕО: ЗАОСТАЛИ НАПОНИ

**Р. Дробњак, А. Седмак,
В. Шијачки-Жеравчић, А. Милосављевић**

Полазећи од основних закона механике континуума, дефинисана је процедура примене методе коначних елемената на проблем одређивања заосталих напона услед каљења, при чему су као улазна величина коришћена временска и просторна расподела температуре, добијена у првом делу рада. Као примена описане процедуре анализирана су два примера одређивања заосталих напона услед каљења цилиндра од челика, у једном случају без фазних трансформација, а у другом случају узимајући у обзир и фазне трансформације типа аустенит - беинит.